JOURNAL OF GEOPHYSICAL RESEARCH, VOL. 91, NO. B6, PAGES 6432-6440, MAY 10, 1986

DOWNDIP TENSIONAL EARTHQUAKES BENEATH THE TONGA ARC: A DOUBLE SEISMIC ZONE ?

Hitoshi Kawakatsu[1]

Department of Geophysics, Stanford University, California

Abstract. Characteristics of seismicity at intermediate depth beneath the Tonga arc are studied. Special attention is paid to newly identified downdip tensional events because the dominance of downdip compression has been known in this area. We reexamine the relatively shallow (<70 km) downdip tensional events, reported in the Harvard centroid moment tensor solutions, by modeling bodywave waveforms of World-Wide Standard Seismograph Network seismograms and conclude that they are in fact intraplate downdip tensional events. Furthermore, these downdip tensional events are consistently located below and seaward of downdip compressional events and appear to constitute a double seismic zone. The result of a relative relocation technique applied to these earthquakes also supports this observation, which was originally based on routinely determined epicenters. The subducting slab beneath the Tonga arc has been considered as a prototype of a compressionally loaded slab. The existence of a double seismic zone in Tonga, therefore, would suggest that double seismic zones, located at intermediate depth in subducting slabs, are more common than previously thought.

Introduction

Kawakatsu [1985a,b] recently reported the presence of a double seismic zone of intermediate depth earthquakes beneath the Tonga arc. Since the subducting slab beneath the Tonga arc has been considered as a prototype of a compressionally loaded slab [e.g., Isacks and Molnar, 1969, 1971; Fujita and Kanamori, 1981], the presence of several downdip tensional events reported by Kawakatsu [1985a,b] is significant, and if there really exists a double seismic zone, it would bring a new aspect to our understanding of the subduction process [Kawakatsu, 1985a]. The purpose of this paper is to show the results of the analysis of the seismicity beneath the Tonga arc, which led the author to conclude the presence of a double seismic zone [Kawakatsu, 1985a,b].

The seismicity of the Tonga-Kermadec area has been studied extensively by many researchers and the most recent and complete summary of the seismicity can be found in the work by Billington [1980]. After selecting well-located earthquakes, she concluded that the thickness of the Wadati-Benioff zone is about 40 km. In the intermediate depth range (70-300 km), the stress state inferred from earthquake focal mechanisms indicates strong downdip compression and downdip tension in the Tonga and Kermadec subduction zones, respectively [Isacks and Molnar, 1971; Billington, 1980; Fujita and Kanamori, 1981]. The activity of deep earthquakes under the Tonga arc is extremely high and the stress state is strongly downdip compressional. Richter [1979] and Giardini and Woodhouse [1984] attributed this to the failure of the slab to penetrate into the lower mantle. Therefore all previous work on the seismicity of the Wadati-Benioff zone under the Tonga arc suggests that the stress pattern of the intermediate depth part of this slab is strongly downdip compressional.

Data presented in this paper show that there are several downdip tensional events and that they are consistently located below and seaward of the downdip compressional events. This is what is expected of a double seismic zone [Hasegawa et al., 1978a,b] and what led the author to infer the presence of a double seismic zone in Tonga. Although there are more downdip compressional events than tensional events in the double seismic zone, the compressional stress (or strain) transmitted from below 200 km depth does not seem to completely overprint and erase the preexisting stress (or strain) feature of a double seismic zone. If we accept the presence of a double seismic zone in Tonga, it suggests that the double seismic zone is a more general and persistent feature of subducting slabs in the intermediate depth range than previously thought and that careful studies of seismicity of other Wadati-Benioff zones will probably reveal other, as yet undiscovered, double seismic zones.

Seismicity

Figure 1 shows a map view of seismicity in the Tonga-Kermadec region with tectonic features. The events are selected from International Seismological Centre (ISC) bulletins under the following conditions: more than 30 observations of P arrivals and depth determined from pP-P time difference. We will call these events "depth-constrained ISC events" and plot them as background seismicity. The numbers in Figure 1 indicate the orientation of great circles connecting a point on the trench and the pole of the arc. The pole of the arc is located at 20.6°N, 102.8°E, so that the 100-km isodepth contour under the Tonga arc of Isacks and Barazangi [1977] is 90° distance from the pole. The pole of the arc is thus chosen to best describe the seismicity in the Tonga region and may not be appropriate for the Kermadec region. In this paper, we focus on the area between azimuths 109° and 116°, where the presence of a double seismic zone is suggested [Kawakatsu, 1985a,b]. A summary of seismicity of the whole area in Figure 1 and a complete list of earthquakes, including events which we will discuss in this paper, can be found in the work by Kawakatsu [1985a].

Depths of earthquakes are, in general, the least well constrained parameters of reported (ISC or Preliminary Determination of Epicenters (PDE)) hypocenters. The relative epicentral location of earthquakes in small areas can, on the other hand, usually be well determined. Therefore it is essential to have accurate depth estimates in order to study the detailed seismicity of shallow and intermediate depth earthquakes in subducting slabs and in order to determine the possible existence of a double seismic zone. The depths of all events used to define the double seismic zone in this study are constrained either by bodywave waveform modeling or surface reflection phases. The epicentral parameters are taken from PDE.

Figures 2 show the cross sections of seismicity between

[1]Now at Seismological Laboratory, California Institute of Technology, Pasadena.

Paper number 5B5690.
0148-0227/86/005B-5690$05.00

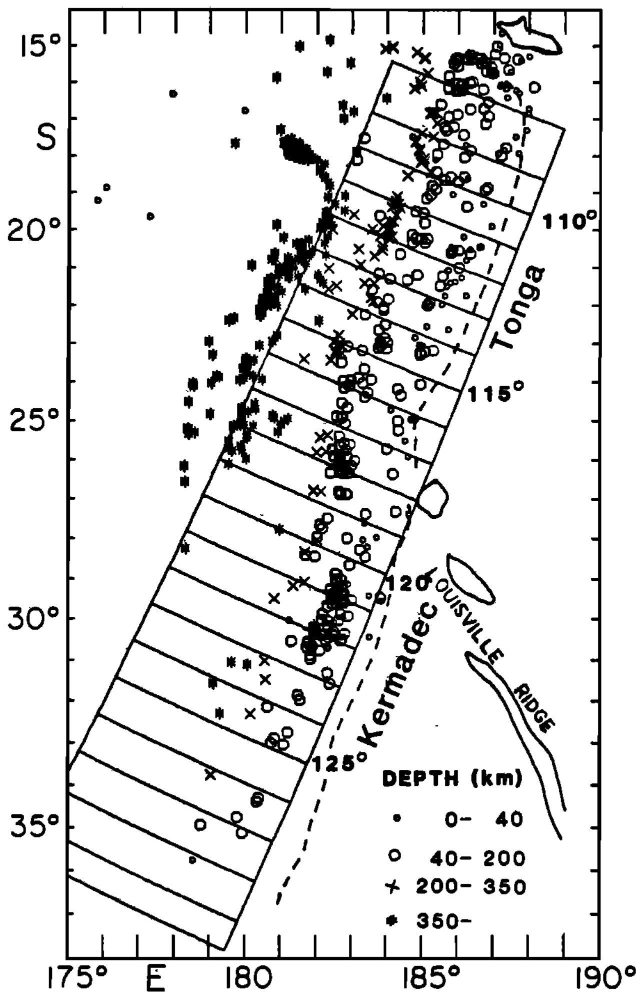

Fig. 1. Map view of the general seismicity of Tonga-Kermadec area. The depth-constrained ISC events are plotted. The dashed line represents the trench. The lines perpendicular to the trench are parts of the great circles which pass through the pole of the arc, and the numbers denote the azimuth of the great circles. The azimuth of these great circles is measured clockwise from north at the pole of the arc. Two lines parallel to the strike of the trench are at distances of 87.5° and 92.5° from the pole.

azimuths 109° and 116°, projected onto planes perpendicular to the strike of the trench. Table 1 summarizes all the downdip tensional events observed in this region. This region is selected because the geometry of the plate defined by seismicity [Isacks and Barazangi, 1977, Figure 2] shows a rather simple planar geometry. North of azimuth 109° (~17.5°S), the end of the subduction zone results in hinge faulting, introducing more complicated stress and strain structure in the slab. South of azimuth 116° (~24.5°S), the lateral bending of the slab near 26°S prevents a simple two-dimensional view of the subduction process. Most events have focal mechanisms of plane strain (or stress) between 50 and 200 km depth and show either downdip tension or compression-type mechanisms, except event H21 (Figure 2f).

Downdip Tensional Events

The difficulties in identifying shallow (<70 km) downdip tensional events come from the fact that their focal mechanisms are similar to those of shallow angle thrust faulting events, which are very common in subduction zones, and that the reported depth estimates are not reliable for this depth range. For example, comparing first-motion P wave waveforms from Honshu, Japan, Seno and Kroeger [1983] found that most of the events that were previously thought to be normal faulting between the Japan trench and the double seismic zone are actually shallow angle thrust events. Therefore it is important to analyze waveforms of those shallow events.

For the Tonga arc, the Harvard centroid moment tensor (CMT) [Dziewonski et al., 1981; Dziewonski and Woodhouse, 1983] catalogue contains three relatively shallow (~60 km) downdip tensional events, H2 (depth=61 km), H26 (57 km), and H49 (70 km). Since all the surface reflections are automatically included in the inversion process, their focal depth estimates should be reliable except for the shallowest events [Dziewonski et al., 1983].

In Figure 3a, the depth of the event H26 is checked by comparing World-Wide Standard Seismograph Network (WWSSN) long-period records and synthetic seismograms at some stations. Synthetic seismograms are calculated by using the program developed by Kroeger and Geller [1980]. PREM [Dziewonski and Anderson, 1981] was used for the structure and the source was located at a depth of 60 km. The early part of the seismogram is best fitted by h=60 km and the later part by a slightly greater depth, suggesting that the shear wave velocity structure in this area is slightly slower than the average value. This supports the reliability of the depth estimates of CMT solution and confirms that this event is an intraplate downdip tensional event. The event H49 is so small that no long-period WWSSN seismogram is available for waveform modeling. The depth could be checked by the WWSSN short-period seismogram only at one station (SPA). The model depth 65 km is slightly shallower than CMT depth, 70 km. Although the first motions are also slightly inconsistent with the CMT solution, it still shows a downdip tensional mechanism.

The depth of the event H2 (June 22, 1977) is controversial [Giardini, 1984]. Although the CMT solution with surface waves gives the depth of 61 km, the CMT solution obtained just from body waves converges to 130 km depth [Giardini, 1984]. The aftershock distribution suggests that the rupture extended down to a depth of 166 km [Silver and Jordan, 1983]. From pP-P readings, Talandier and Okal [1979] estimated the focal depth to be shallower than 50 km. The generation of tsunamis indicates that the rupture extended to shallow depths, and the excitation of overtones of normal modes suggests the source has to be deeper than 100 km (E. A. Okal, personal communication, 1984). Christensen and Lay [1985] recently reported a depth of 70 km from body wave waveform analysis and suggested that this event was associated with the subduction of the Louisville Ridge. The rupture process seems to be very complicated, but at least there must be a major rupture extending deeper than the depth given by the CMT solution. Although the CMT depth is used here, it probably underestimates the depth of this large normal faulting event ($M_0=1.4\times10^{28}$ dyn cm). Although this event may be spatially as large as the entire thickness of the "brittle" portion of the lithosphere, we do not think that this was the case because a downdip compressional-type event (C4, Table 2) occurred in the same area several months prior to the occurrence of this event. The occurrence of the downdip compressional event is not consistent with the idea that the whole lithosphere is under downdip tensional stress state.

The presence of the above mentioned shallow (~60 km) downdip tensional events and two deeper downdip tensional events (F41 and F72) shows that there are downdip

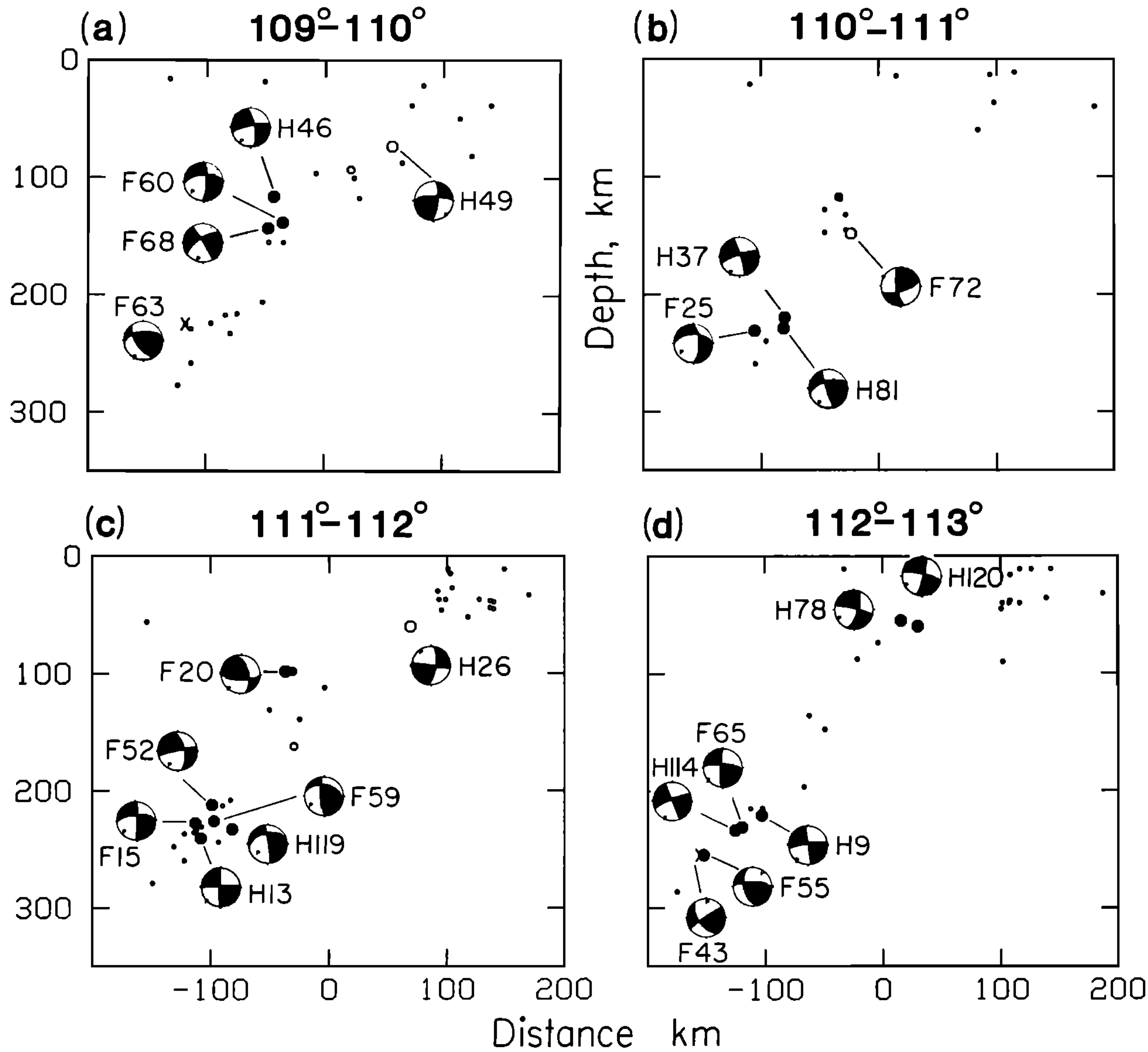

Fig. 2. Cross sections perpendicular to the trench. Large and medium-sized symbols represent events for which focal mechanism solutions are available and for which only mechanism types can be determined, respectively. Open and solid circles denote downdip tensional and downdip compressional events, respectively. Crosses are the events which show neither of those mechanisms. The nearside of the focal hemisphere is also plotted. Small dots are the depth-constrained ISC events. The numbers on the top of each figure correspond to the azimuth range of each of the cross section. The horizontal scale is a degree along the great circle perpendicular to the strike of the trench.

tensional events in this region where downdip compressional stress had been thought to dominate the whole slab and that more likely these two different kinds of earthquakes make up a double seismic zone. Although all the events for which focal mechanism can be determined have been already studied, there are still several more earthquakes which by using P wave first motion and S wave polarization of WWSSN records, it is possible to classify as downdip tensional or downdip compressional types, on the assumption that each earthquake must be one of the two types.

Figure 4 shows the lower hemisphere of the focal sphere of the events for which the type of mechanism can be determined. Events T1, T2, and T3 are classified as downdip tensional type and events C1, C2, C3, C4, and C5 are classified as downdip compressional type (Table 2). Figure 5 summarizes all the results. It is clear that all the compressional events are consistently located above all the tensional events and they appear to constitute a double seismic zone.

Relocation

Relative errors in routine epicentral estimates (e.g., ISC, PDE) are believed to be much smaller than errors in absolute coordinates. It is, however, not appropriate to use the reported standard deviations as true values of the relative errors in the epicentral parameters. This is because the set of stations used to locate each event is different and because errors due to the differences between the assumed earth structure and the real structure enter into the location process differently from station to station and event to event.

In order to investigate the possibility that the separa-

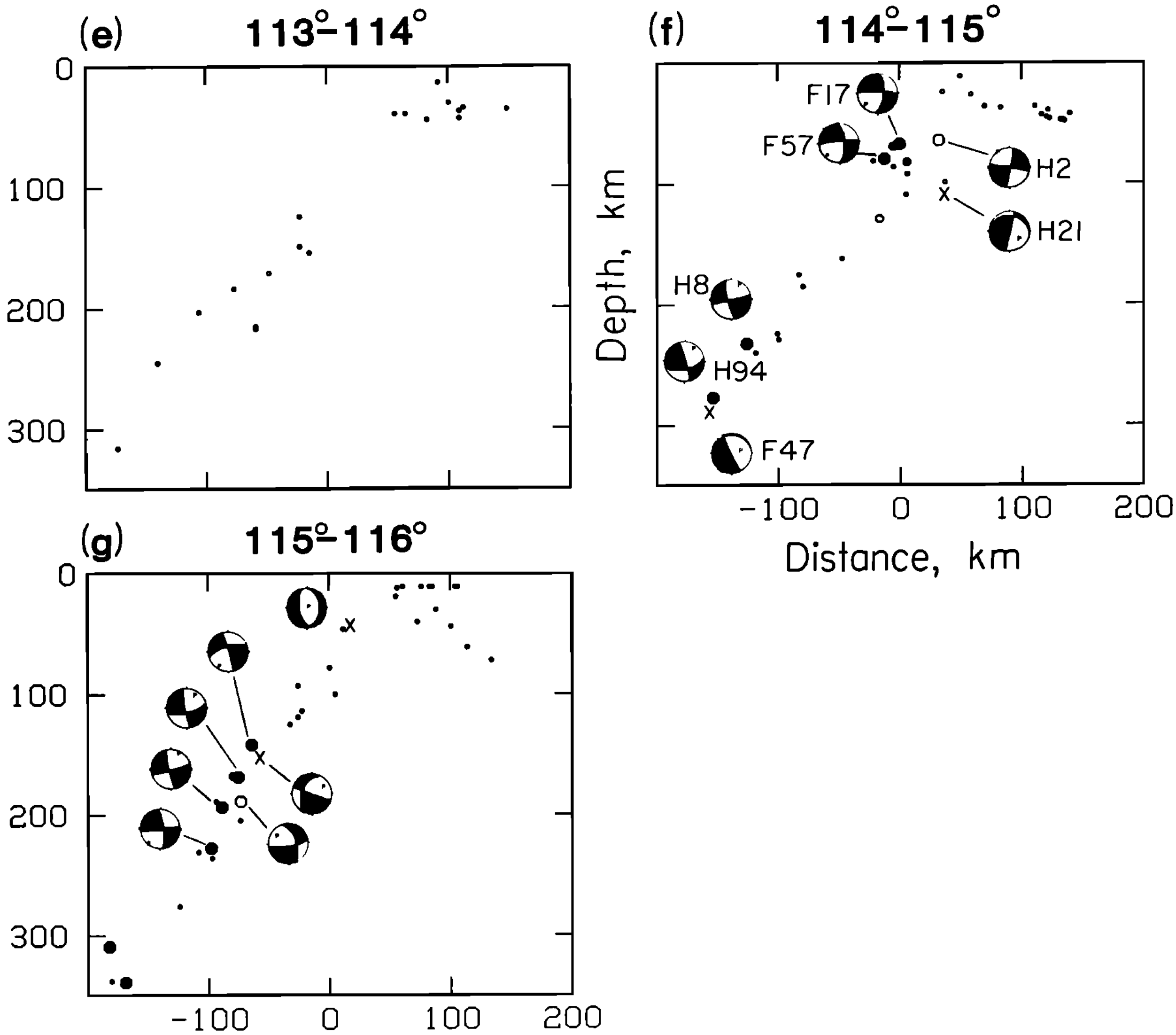

Fig. 2. (continued)

tion of the two seismic zones seen in Figure 5 is fortuitous, a relative relocation of the events is performed. The result supports the presence of the double seismic zone.

Data

Earthquakes are selected from the ISC bulletin from 1971 to 1979 with the following conditions: (1) depths between 60 km and 200 km constrained by pP-P phase, (2) more than 30 P arrival observations, and (3) azimuth between 107° and 117° (Figure 1).

The first condition assures that the least well constrained parameter (depth) is constrained by pP-P time. The estimates of station residuals will therefore be more reliable than those obtained without depth constraints. The second criterion is needed to obtain reliable statistical error estimates. In total, 46 earthquakes were selected, including 13 events for which either focal mechanism or focal mechanism type is determined.

Relocation Procedure

The relocation procedure is similar to those done by Veith [1974] and Samowitz and Forsyth [1981]. The pur-

TABLE 1 Downdip Tensional Events

Event	Date	Latitude, deg	Longitude, deg	Depth, km	m_b	Distance deg	Az deg	P Axis Pl	P Axis Az	T Axis Pl	T Axis Az	Strike	Dip	Strike	Dip	Reference
F41	Aug 15, 1968	-23 78	182 58	186	5 5	0 65	115 78	32	72	56	268	78	348	14	141	Billington [1980]
F72	Aug 28, 1971	-18 81	185 30	145	5 4	0 20	110 22	29	109	50	336	80	40	27	153	Kawakatsu [1985a]
H2	June 22, 1977	-22 88	184 10	61	6 8	-0 30	114 42	56	107	34	286	11	14	79	197	CMT solution
H26	Nov 4, 1981	-20 05	185 72	57	6 3	-0 63	111 23	53	87	37	273	8	19	82	180	CMT solution
H49	July 30, 1982	-18 45	186 26	70	5 5	-0 52	109 55	47	116	36	258	21	291	84	185	CMT solution

Az, azimuth, pl, plunge Distance and azimuth are given in degrees Distance is given by (90° -(distance from the pole of the arc)) and azimuth is measured at the pole of the arc from north

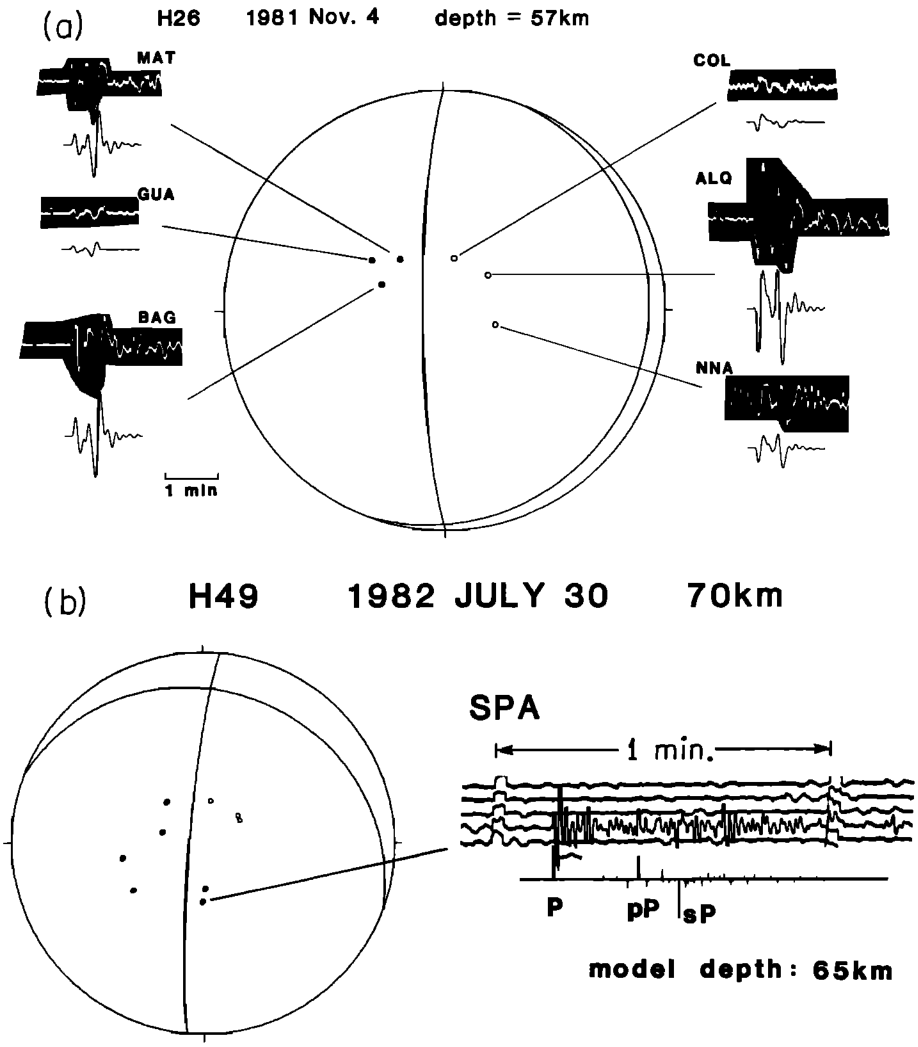

Fig. 3. Synthetic seismograms are compared with WWSSN seismograms to check the depth of events (a) H26 and (b) H49. The focal mechanisms are those of the CMT solutions. The model depths are (a) 60 km and (b) 65 km, while the CMT depths are (a) 57 km and (b) 70 km.

pose is, however, slightly different. The purpose here, as mentioned above, is to obtain proper relative error estimates of epicentral parameters, so that the apparent separation of the two seismic zones can be tested.

The basic assumption is that the ray paths from earthquakes in some small region to a particular station at teleseismic distance (>30°) are similar and thus the travel time residuals due to earth model error are similar for each station. Under these assumptions, the master event technique and joint hypocenter determination technique (JHD [Douglas, 1967; Dewey, 1972]) have been introduced. The region of interest in this paper is large (~800 km along the strike of the Tonga trench), and the above conditions may not be fulfilled. Following Samowitz and Forsyth [1981], we assume that the travel time residuals to a given station (due to the earth model error) vary smoothly as a function of distance between the station and earthquakes and can be modeled linearly to the first order.

There are two steps in the relocation procedure. For each step, the earthquake location program originally writ-

TABLE 2. Events With Mechanism Type (Figure 4)

Event	Date	Time	Latitude, deg	Longitude, deg	Depth, km	m_b	Distance, deg	Azimuth, deg
T1	Agu. 12, 1966	0359:49.7	-22.40	183.80	127	5.4	0.14	114 08
C1	Agu. 8, 1968	1115:46.3	-20.03	184.69	96	5.5	0.27	111.57
T2	Agu. 29, 1972	0559:01.7	-19.99	184.72	160	5.4	0.26	111.52
C2	Nov. 11, 1974	0629:21.1	-23.91	182.44	166	5.6	0.71	115.95
C3	May 5, 1975	2028:08.3	-23.01	183.76	80	5.6	-0.06	114.66
T3	March 26, 1977	081918.5	-18.58	185.85	91	5.6	-0.20	109.82
C4	Feb. 22, 1978	1937:17.0	-22.70	183.79	67	5.6	0.04	114.36
C5	May 27, 1980	1301:34.8	-18.65	185.25	115	6.1	0.30	110 09

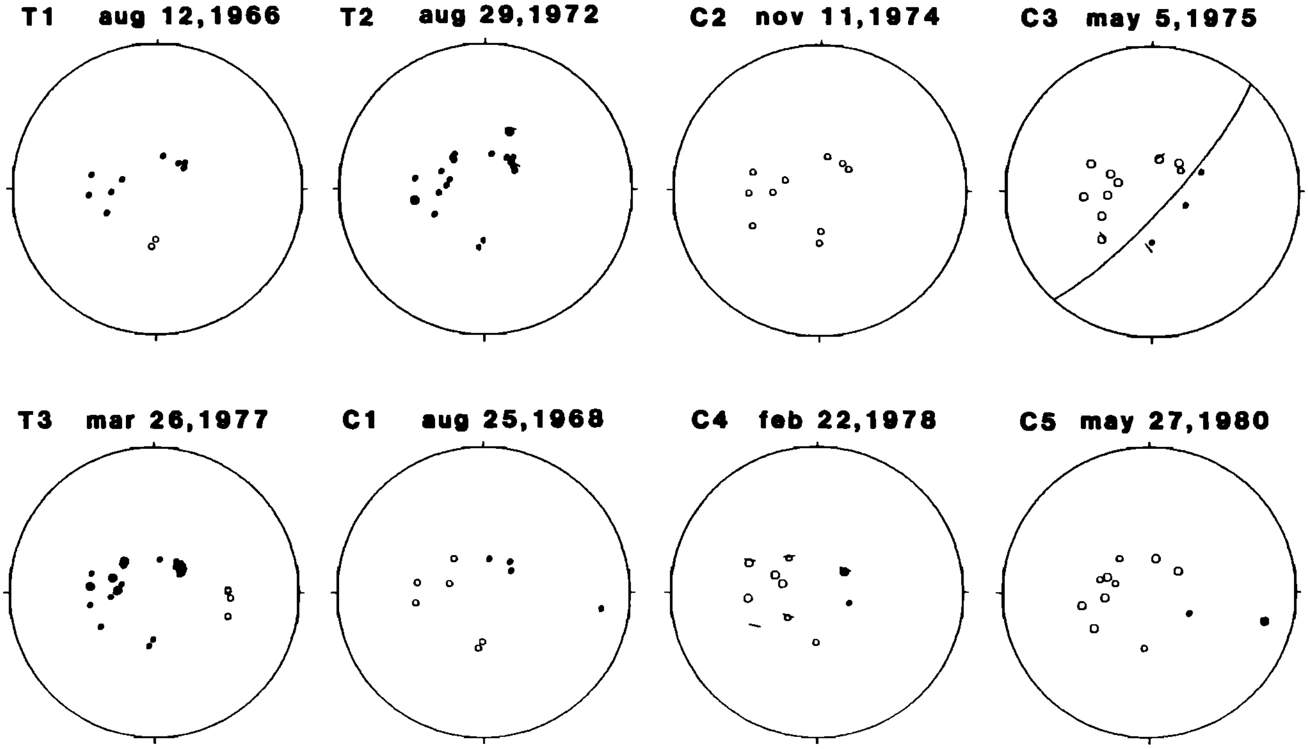

Fig. 4. Events for which only the type of focal mechanism can be determined (Table 2). First-motion data from long- and short-period WWSSN records are plotted on the focal sphere. The large and small circles correspond to long- and short-period data, respectively. Asterisks denote near-node first motions.

ten by Dewey (JHD77 [Dewey, 1972]) was used with some modification. Although JHD77 is a program for the joint hypocenter determination, it is used simply as an epicenter estimation program (depths are determined by pP-P time difference).

For the first step, the earthquakes are relocated using the P wave arrival times reported at station distances between 30° and 100° in order to estimate the station correction term in the residuals. After the earthquakes are relocated, the stations which have arrivals from more than 10 earthquakes are selected for the next step. There are 113 stations left at this stage. The travel time corrections for these stations are determined by least squares fit of the residuals to a linear function of distance between the stations and earthquakes (Figure 6).

In the second step, the travel times are first subtracted by the amount estimated from the linear function obtained in the first step. Relocation was then performed for each event separately using only the arrivals from those 113 stations. Each station was weighted inversely proportionally to its residual variance estimated in the first step. Crosses in Figure 6 denote the residuals after the second step and are distributed around the solid lines. Further steps (i.e., reestimating the station correction terms and repeating the second step) will not affect the result significantly because the station correction terms do not change significantly.

Result

The results are summarized in Figures 7 and 8. Figure 7 shows the cross sections of the results of relocation at each step. After the second step, Figure 7c shows the separation of the two zones. The horizontal bars denote the estimated 90% confidence intervals from Student t statistics, and the distance of separation exceeds the error bars significantly. In Figure 7d, both downdip compression and tension events are located consistently on the upper and the lower plane of the double seismic zone, respectively. The error estimate here does not include the error introduced by the fact that all the earthquakes (located in a 700-km-long zone parallel to the trench) are plotted on the same cross section. Therefore what is important is that the downdip compressional events are still located consistently above the downdip tensional events even after the relocation.

The two zones become closer after the relocation, but this is expected for the following reason. The effect of the variation of thermal structure within the slab [e.g., Sleep, 1973] on body wave travel times is not considered in the relocation process [Engdahl and Fujita, 1981; Fujita et al., 1981]. As pointed out by Engdahl and Fujita [1981], this

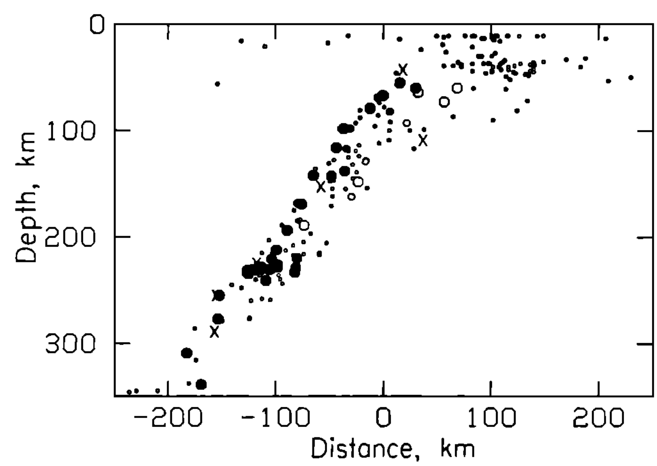

Fig. 5. Cross section of the all the events between azimuth 109° and 116°. The symbols are the same as in Figure 2.

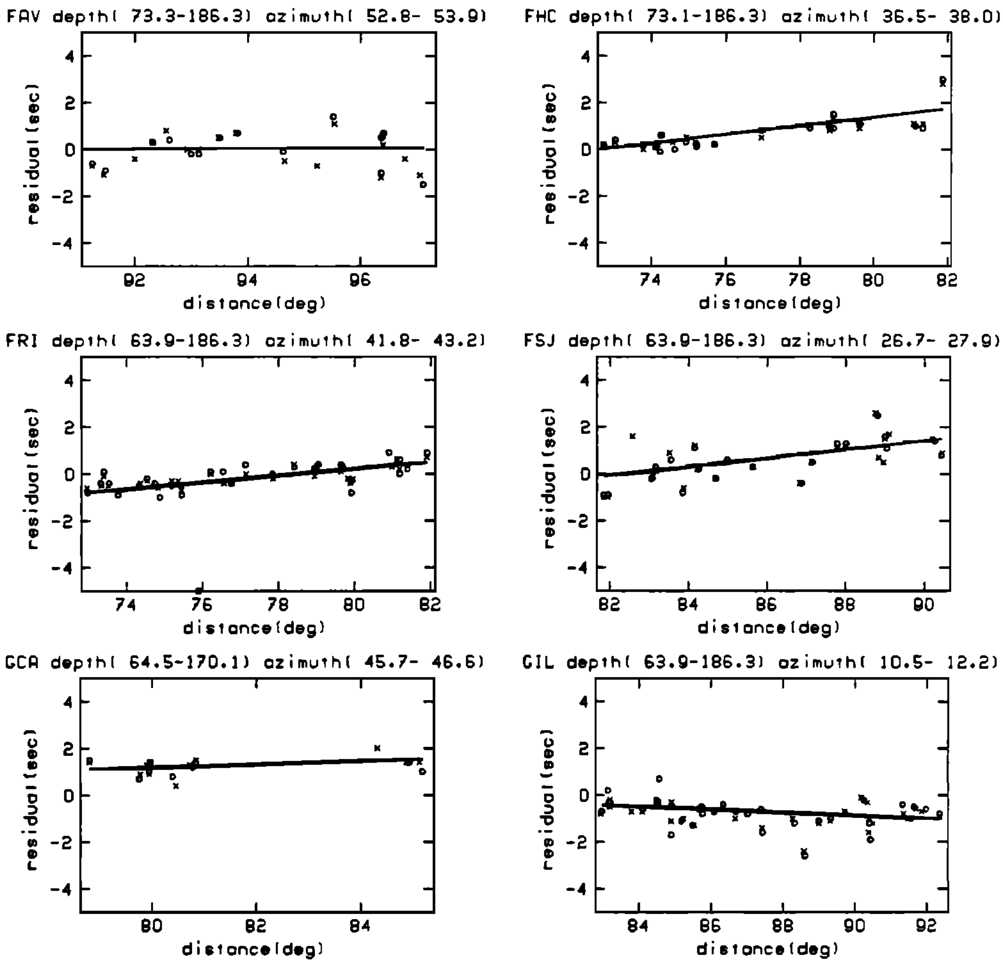

Fig. 6. Examples of station arrival time residuals and the distance dependent station travel time corrections. Open circles and crosses denote residuals after the first and the second step of the relocation, respectively. Solid straight line is the travel time correction for the station, estimated from the open circles by a least squares method.

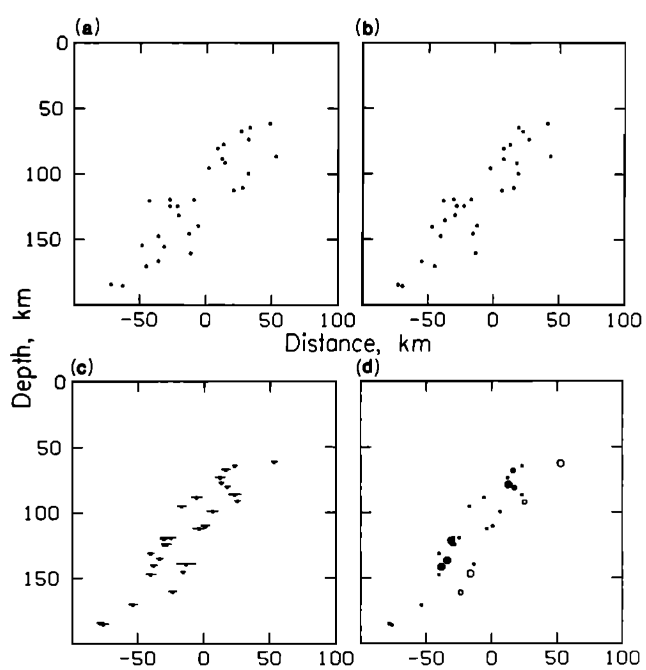

Fig. 7. Results of relocation. (a) Original ISC location. (b) After the first iteration. (c) After the second iteration. The horizontal bars denote 90% confidence intervals from Student t statistics. (d) The final result with focal mechanism types. Note that the downdip compressional events are still located above the downdip tensional-type events. The symbols are the same as in Figure 2.

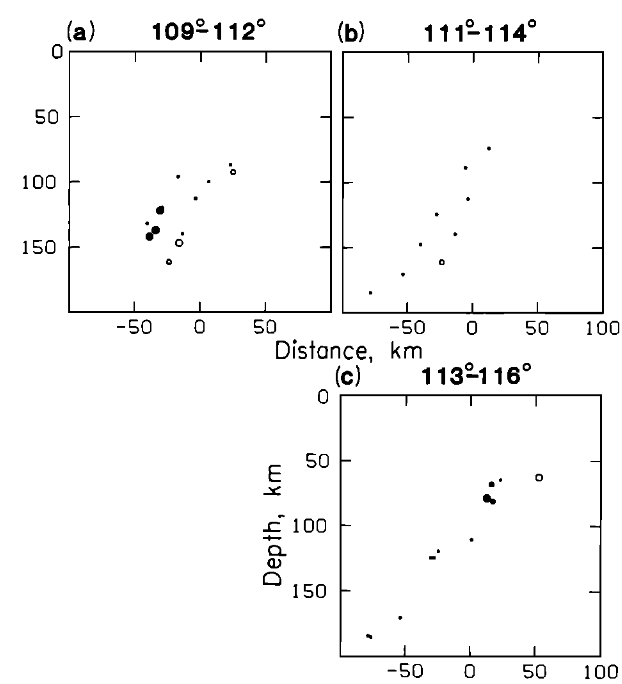

Fig. 8. More results of the relocation. Cross sections between (a) azimuth 109°-112°, (b) 111° - 114°, (c) 113°-116°. Note that the downdip compressional and the downdip tensional events are still located in the upper and lower edge of the seismic zone in each cross section. The symbols are the same as in Figure 2.

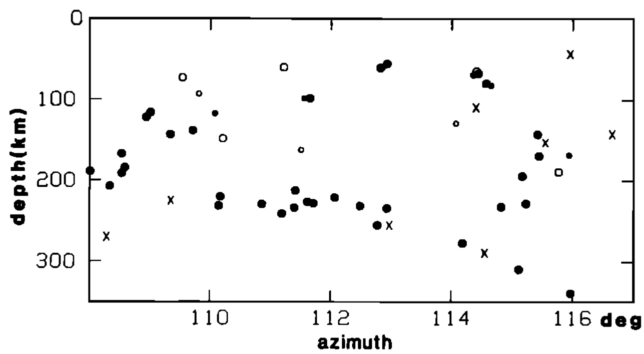

Fig. 9. Cross section parallel to the strike of the trench. All the intermediate depth events for which either focal mechanisms (large mark) or focal mechanism types (smaller mark) are available are plotted. The symbols are the same as in Figure 2.

effect can be as significant as the station correction itself. However, ignoring this effect tends to move the locations of the events of the lower plane (i.e., downdip tensional) to the dip direction of the slab relative to the events of the upper plane [see Fujita et al., 1981, Figure 10]. When the depth is constrained in the location process, this causes the horizontal migration of events in the lower plane toward the upper plane. Therefore the separation of two planes should be actually greater than that shown.

In Figures 8a, 8b, and 8c, the cross sections of the narrower (~300 km wide) sections are plotted to show that the apparent separation of the two seismic zones cannot be attributed to the way the data are plotted.

Discussion

Both the earthquake focal mechanisms and the results of the relocation in the previous section support the existence of the double seismic zone. The cross section parallel to the strike of the trench between azimuth 108° and 117° (Figure 9) shows some regional variation. There is a lack of downdip tensional and downdip compressional events in the region between azimuth 111.5° and 114° and in the region between 110° and 111.5°, respectively. This may be due to insufficient sample size. The temporal variation of seismicity due to the state of stress at the thrust zone can also cause similar effects, as suggested by Kawakatsu and Seno [1983]. What is important is that both downdip tensional events and downdip compressional events occur where they are expected to occur if there is a double seismic zone.

As seen in Figure 9, there are many downdip compressional events directly downdip beneath the double seismic zone. The deeper part of this slab is also known to be the most active of all the subduction zones in the world [e.g., Giardini and Woodhouse, 1984]. Thus it is reasonable to think that no other slab has stronger support from below 200 km depth than the intermediate depth part of the slab in Tonga. Although there are more downdip compressional events than downdip tensional events, there appears to exist a double seismic zone in Tonga. This suggests that in any currently observed subducting slab, compressional stress or strain (either due to inability of the slab to penetrate into the lower mantle or to the strong viscous resistance to the subduction in the mesosphere) transmitted from below 200 km depth cannot overprint completely and erase the preexisting stress feature of a double seismic zone.

The discovery of this double seismic zone and the nature of deep earthquake activity beneath it suggest that double seismic zones are a common and persistent feature of subducting slabs and that there may be many other undiscovered double seismic zones in other subduction zones. This point and the origin of double seismic zones are discussed in a separate paper [Kawakatsu, 1986].

Acknowlegments. I thank Bob Geller, Eric Peterson, and Rob Haar for reading the manuscript. Comments by J. Dewey and an anonymous reviewer also improved the manuscript This work was supported by National Science Foundation grants EAR82-18961 and EAR83-06555.

References

Billington, S., The morphology and tectonics of the subducted lithosphere in the Tonga-Fiji-Kermadec region from seismicity and focal mechanism solutions, Ph.D. thesis, 220 pp., Cornell Univ., Ithaca, N. Y., 1980.

Christensen, D., and T. Lay, Large earthquakes associated with subduction of the Louisville ridge, Eos Trans. AGU, 66, 298, 1985.

Dewey, J. W., Seismicity and tectonics of western Venezuela, Bull. Seismol. Soc. Am., 62, 1711-1751, 1972.

Douglas, A., Joint epicenter determination, Nature, 215, 47-48, 1967.

Dziewonski, A. M., and D. L. Anderson, Preliminary reference earth model (PREM), Phys. Earth Planet. Inter., 25, 297-356, 1981.

Dziewonski, A. M., and J. H. Woodhouse, An experiment in systematic study of global seismicity: centroid-moment tensor solutions for 201 moderate and large earthquakes of 1981, J. Geophys. Res., 88, 3247-3271, 1983.

Dziewonski, A. M., T. A. Chou, and J. H. Woodhouse, Determination of earthquake source parameters from waveform data for studies of global and regional seismicity, J. Geophys. Res., 86, 2825-2852, 1981.

Dziewonski, A. M., A. Friedman, D. Giardini, and J. H. Woodhouse, Global seismicity of 1982: Centroid-moment tensor solutions for 308 earthquakes, Phys. Earth Planet. Inter., 33, 76-90, 1983.

Engdahl, E. R., and K. Fujita, Comment on "Double seismic zone beneath the Mariana Island arc" by Ilene R. Samowitz and Donald W. Forsyth, J. Geophys. Res., 86, 7023-7024, 1981.

Fujita, K., and H. Kanamori, Double seismic zones and stresses of intermediate depth earthquakes, Geophys. J. R. Astron. Soc., 66, 131-156, 1981.

Fujita, K., E. R. Engdahl, and N. H. Sleep, Subduction zone calibration and teleseismic relocation of thrust zone events in the Central Aleutian islands, Bull. Seismol. Soc. Am., 71, 1805-1828, 1981.

Giardini, D., Systematic analysis of deep seismicity: 200 centroid-moment tensor solutions for earthquakes between 1977 and 1980, Geophys. J. R. Astron. Soc., 77, 883-914, 1984.

Giardini, D., and J. H. Woodhouse, Deep seismicity and modes of deformation in Tonga subduction zone, Nature, 307, 505-509, 1984.

Hasegawa, A., N. Umino, and A. Takagi, Double-planed structure of the deep seismic zone in the northeastern Japan arc, Tectonophysics, 47, 43-58, 1978a.

Hasegawa, A., N. Umino, and A. Takagi, Double-planed deep seismic zone and upper-mantle structure in the northeastern Japan arc, Geophys. J. R. Astron. Soc., 54, 281-296, 1978b.

Isacks, B. L., and M. Barazangi, Geometry of Benioff zones. Lateral segmentation and downwards bending of the subducted lithosphere, in Island Arcs, Deep Sea Trenchs and Back-Arc Basins, Maurice Ewing Ser., vol. 1, edited by M. Talwani and W. C. Pitman III, pp. 99-114, AGU, Washington, D. C., 1977.

Isacks, B. L., and P. Molnar, Mantle earthquake mechanisms and the sinking of the lithosphere, Nature, 223, 1121-1124, 1969.

Isacks, B. L., and P. Molnar, Distribution of stresses in the descending lithosphere from a global survey of focal-mechanism solutions of mantle earthquakes, Rev. Geophys., 9, 103-174, 1971.

Kawakatsu, H., Double seismic zones: a first order feature of plate tectonics, Ph.D. thesis, Stanford Univ., Stanford, Calif., 1985a.

Kawakatsu, H., Double seismic zone in Tonga, Nature, 316, 53-55, 1985b.

Kawakatsu, H., Double seismic zones: Kinematics, J. Geophys. Res., in press, 1986.

Kawakatsu, H., and T. Seno, Triple seismic zone and the regional variation of seismicity along the northern Honshu arc, J. Geophys. Res., 88, 4215-4230, 1983.

Kroeger, G. C., and R. J. Geller, Modeling of teleseismic body waves from submarine earthquakes in a vertically heterogeneous crust, Eos Trans. AGU, 61, 301, 1980.

Richter, F. M., Focal mechanisms and seismic energy release of deep and intermediate earthquakes in the Tonga-Kermadec region and their bearing on the depth extent of mantle flow, J. Geophys. Res., 84, 6783-6795, 1979.

Samowitz, I. R., and D. W. Forsyth, Double seismic zone beneath the Mariana Island arc, J. Geophys. Res., 86, 7013-7021, 1981.

Seno, T., and G. C. Kroeger, A reexamination of earthquakes previously thought to have occurred within the slab between the trench axis and double seismic zone, northern Honshu arc, J. Phys. Earth, 31, 195-216, 1983.

Silver, P. G., and T. H. Jordan, Total-moment spectra of fourteen large earthquakes, J. Geophys. Res., 88, 3273-3293, 1983.

Sleep, N. H., Teleseismic P-wave transmission through slabs, Bull. Seismol. Soc. Am., 63, 1349-1373, 1973.

Talandier, J., and E. A. Okal, Human perception of T waves: The June 22, 1977 Tonga earthquake felt on Tahiti, Bull. Seismol. Soc. Am., 69, 1475-1486, 1979.

Veith, K., The relationship of island arc seismicity to plate tectonics, Ph.D. thesis, South. Methodist Univ., Dallas, Tex., 1974.

H. Kawakatsu, Seismological Laboratory 252-21, California Institute of Technology, Pasadena, CA 91125.

(Received June 24, 1985;
revised November 21, 1985;
accepted January 24, 1986.)